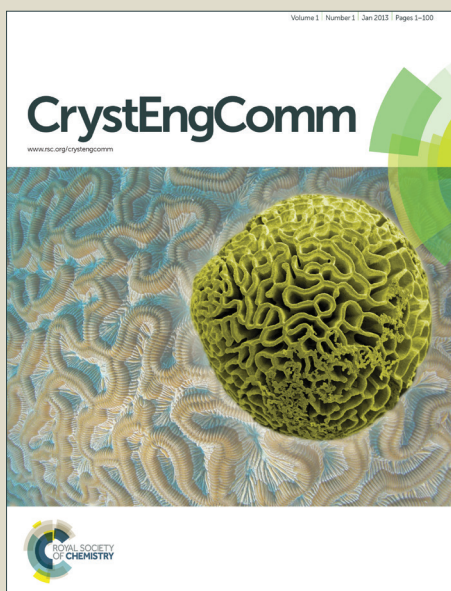


# CrystEngComm

Accepted Manuscript



This is an *Accepted Manuscript*, which has been through the Royal Society of Chemistry peer review process and has been accepted for publication.

*Accepted Manuscripts* are published online shortly after acceptance, before technical editing, formatting and proof reading. Using this free service, authors can make their results available to the community, in citable form, before we publish the edited article. We will replace this *Accepted Manuscript* with the edited and formatted *Advance Article* as soon as it is available.

You can find more information about *Accepted Manuscripts* in the [Information for Authors](#).

Please note that technical editing may introduce minor changes to the text and/or graphics, which may alter content. The journal's standard [Terms & Conditions](#) and the [Ethical guidelines](#) still apply. In no event shall the Royal Society of Chemistry be held responsible for any errors or omissions in this *Accepted Manuscript* or any consequences arising from the use of any information it contains.

## Growth, thermal, and spectroscopic properties of a 2.911 $\mu\text{m}$ Yb,Ho:GdYTaO<sub>4</sub> laser crystal

Renqin Dou,<sup>a,b</sup> Qingli Zhang,<sup>\*a</sup> Dunlu Sun,<sup>a</sup> Jianqiao Luo,<sup>a</sup> Huajun Yang,<sup>a,c</sup> Wenpeng Liu<sup>a</sup> and Guihua Sun<sup>a</sup>

<sup>a</sup> The Key Laboratory of Photonic Devices and Materials, Anhui Institute of Optics and Fine Mechanics, Chinese Academy of Sciences, Hefei, Anhui, 230031, PR China

<sup>b</sup> University of Science and Technology of China, Hefei 230026, PR China

<sup>c</sup> University of Chinese Academy of Sciences, Beijing, 100049, PR China

### Abstract

A promising 2.911  $\mu\text{m}$  Yb,Ho:GdYTaO<sub>4</sub> laser crystal has been grown successfully by the Czochralski method for the first time. The crystal belongs to the monoclinic space group of  $I_{2/a}$  (No.15) and high crystalline quality is demonstrated by X-ray rocking curves. The effective segregation coefficient  $k_{eff}$  of Yb, Ho, and Y are 1.08, 0.96, and 0.9, respectively, all close to 1. Crystal density is measured to be 8.59 g cm<sup>-3</sup> by the buoyancy method. Thermal property indicates that the Yb,Ho,Y:GdTaO<sub>4</sub> crystal should be pumped along  $c$ -axis in order to reduce the thermal lensing effect. Strong absorption in the range of 900-1000 nm and emission at 2911 nm are obtained in the as-grown crystal. In comparison with corresponding level lifetimes of Yb,Ho:YSGG, Tm,Ho:LuAG, Tm,Ho:YAG, and Ho:YAG, the Yb,Ho,Y:GdTaO<sub>4</sub> crystal exhibits a relatively shorter lifetime 7.298 ms for lower laser level <sup>5</sup>I<sub>7</sub> and longer lifetime 419  $\mu\text{s}$  for upper laser level <sup>5</sup>I<sub>6</sub>, which are very beneficial to realize population inversion and laser output.

### 1. Introduction

The new lasers at wavelength range from 2.7 to 3.0  $\mu\text{m}$  have been widely attracted by the requirements for medical, biological, and remote sensing applications due to their strong absorption in water, biological tissues, and vapor.<sup>1-2</sup> However, the fine spectral structure in the range of 2.7-3.0  $\mu\text{m}$  shows the water absorption at the wavelength of 2.911  $\mu\text{m}$  is weak. Therefore, the 2.911  $\mu\text{m}$  laser has less absorption loss<sup>3</sup> when it transmits in the atmosphere, which can be applied in the fields of the detection, military, and scientific research. Numerous studies<sup>4-9</sup> have reported the 2.7-3.0  $\mu\text{m}$  lasers generated by Er-doped laser crystals with <sup>4</sup>I<sub>11/2</sub>→<sup>4</sup>I<sub>13/2</sub> transition. Another possibility of generating 2.7-3.0  $\mu\text{m}$  radiation is the <sup>5</sup>I<sub>6</sub>→<sup>5</sup>I<sub>7</sub> transition of Ho<sup>3+</sup>, which possesses rich energy levels.<sup>10-11</sup>

In 2014 Zhang *et al.* reported that a emission peak of Tm,Ho:LuAG (Lu<sub>3</sub>Al<sub>5</sub>O<sub>12</sub>) laser crystal is located at 2.913  $\mu\text{m}$ , which is close to 2.911  $\mu\text{m}$ . Aiming at finding new 2.911  $\mu\text{m}$  laser crystals, we focus on the properties of Ho<sup>3+</sup>-doped GdTaO<sub>4</sub> (GTO) crystal. The GTO material was attracted because of its scintillation properties<sup>12-14</sup> and was also studied as laser host by our group due to its low symmetry and strong crystal

\* Corresponding author. Tel./fax: +86-551-65591039, E-mail address: zql@aiofm.ac.cn

field effect.<sup>15-17</sup> In the preliminary work, the Tm,Ho:GTO polycrystalline powder showed no 2.911  $\mu\text{m}$  emission peak. Failing in Tm sensitized Ho-doped GTO crystal, we used Yb as the sensitizer. Fortunately, 2.911  $\mu\text{m}$  emission peak is obtained in Yb,Ho-doped GTO through tuning crystal field by the doping of  $\text{Y}^{3+}$  ions.

In this paper, Yb,Ho:GdYT<sub>2</sub>O<sub>7</sub> (Yb,Ho:GYTO) crystal is grown by the Cz method. The crystal structure, crystalline quality, and components are analyzed. Thermal properties, including the specific heat, thermal expansion, and thermal conductivity, are investigated. In addition, the optical properties related to the laser performance are also studied and discussed.

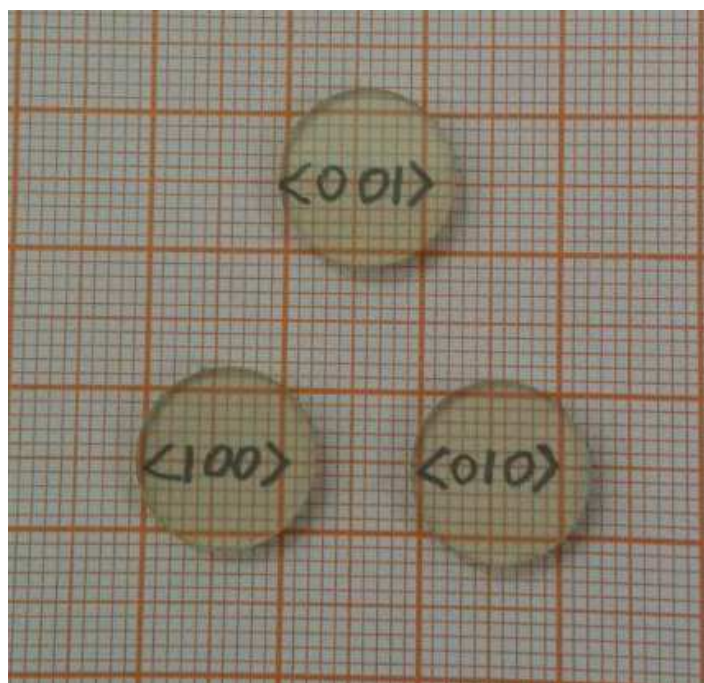
## 2. Experimental

### 2.1 Crystal growth

Yb,Ho:GYTO crystals were grown by the Czochralski method. The processes of crystal growth are similar to those reported in Ref. 12 and 13. Starting materials were prepared from the oxides of Yb<sub>2</sub>O<sub>3</sub> (5N), Ho<sub>2</sub>O<sub>3</sub> (5N), Gd<sub>2</sub>O<sub>3</sub> (5N), Y<sub>2</sub>O<sub>3</sub> (5N), and Ta<sub>2</sub>O<sub>5</sub> (4N). The oxides were weighed according to the chemical formula Yb<sub>0.05</sub>Ho<sub>0.01</sub>Gd<sub>0.74</sub>Y<sub>0.2</sub>TaO<sub>7</sub>. After being mixed thoroughly and pressed into disks, the oxides were loaded into an iridium crucible and melted in a JGD-60 furnace (CETC26<sup>th</sup>, China) with an automatic diameter controlled system. Using an *a*-axis oriented single crystal GdTaO<sub>4</sub> (GTO) bar as seed, the crystals were grown in a nitrogen atmosphere with a rotation speed of 5–8 rpm and pulling rate of 0.5–1 mm/h. As shown in Fig. 1.(a), a transparent crystal with a size of  $\Phi$  23 mm  $\times$  40 mm was obtained. The samples of  $\Phi$  12.7 mm  $\times$  2.5 mm were cut separately from the post-annealed crystal for measurements (shown in Fig. 1.(b)).



(a)



(b)

**Fig. 1** (a) Photograph of the as-grown Yb, Ho:GYTO crystal. (b)  $\langle 100 \rangle$ ,  $\langle 010 \rangle$ , and  $\langle 001 \rangle$  oriented wafers of Yb, Ho:GYTO crystal.

## 2.2 Characterization

The doping concentrations of Yb, Ho, and Y in the shoulder part of Yb, Ho:GYTO crystal were measured with an X-ray fluorescence spectrometer (XRF). Compared with starting materials used for crystal growth, the effective segregation coefficient ( $k_{eff}$ ) was calculated. The XRD patterns of Yb, Ho:GYTO crystal were measured using a Philips X'pert PRO X-ray diffractometer and employing Cu K $\alpha$  radiation ( $\lambda=1.540598$  Å). The diffraction data were recorded in the  $2\theta$  range of  $10-90^\circ$  with the scan step of  $0.033^\circ$ . The rocking curves were collected by a high resolution X'pert Pro MPD diffractometer equipped with a Hybrid K $\alpha$ 1 monochromator. Thermal expansion behavior of crystals along  $a$ ,  $b$ , and  $c$  axes were measured in the temperature range of 300-893 K using a DIL-402C thermal dilatometer with a heating rate of 5 K/min. The samples coated with graphite were used for the measurements of specific heat and thermal diffusivity along the  $a$ ,  $b$ , and  $c$  axes by a Laser Flash Apparatus (LFA457). The absorption spectra of crystals with  $a$ ,  $b$ , and  $c$  axes were recorded by a spectrophotometer (PE lambda 950) in the wavelength range of 400 to 3000 nm. A fluorescence spectrometer (Edinburgh FLSP920) with an excitation source of 940 nm LD and OPO (Opolette 355I) laser were used to measure the fluorescence spectra and the fluorescence decay curves.

## 3. Results and discussion

### 3.1 Crystal growth, structure characterization, components analysis and crystalline quality

As mentioned in Ref. 13, there are several challenges in the growth of GTO crystal, such as phase transition at about 1400 °C, cracking and cleaving along the (010) plane, and high melting point. The melting point of Yb,Ho:GdYTaO<sub>4</sub> crystal is about 1950 °C measured by infrared thermometer (Raytek, 3i). Therefore, it is harder to gain Yb,Ho:GYTO crystal for the doping. From our repeatedly growth experience, a good thermal field is favorable for growing high quality Yb,Ho:GYTO crystal. To reduce the crack, the cooling process is divided into several segments. Through optimizing the temperature gradient and designing the cooling process, using *a*-axis seed, a relatively high quality of crack-free and transparent Yb,Ho:GYTO crystal is obtained successfully. Fig. 1 (a) and (b) show the as-grown Yb,Ho:GYTO crystal and the polished wafers of Yb,Ho:GYTO crystal, respectively. There are no cracks and low angle boundaries in the as-grown Yb,Ho:GYTO crystal. Under a 1W 532 nm laser, no light-scattering pellets are observed. These results indicate that the as-grown Yb,Ho:GYTO crystals have good optical quality and are suitable for laser experiments.

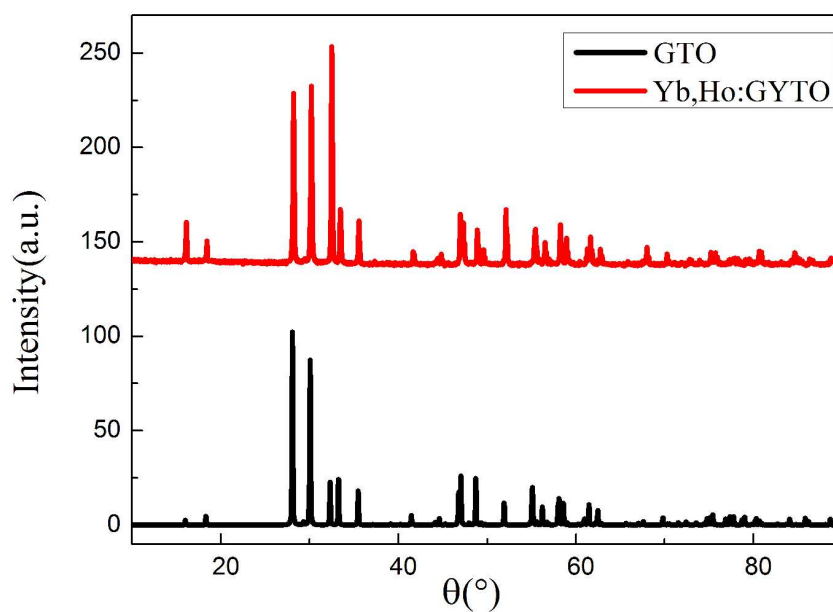


**Fig. 2** XRD diffraction patterns of the as-grown Yb,Ho:GYTO crystal and GTO standard patterns (ICSD # 153362).

The XRD patterns of Yb,Ho:GYTO and GTO are shown in Fig. 2. Strong diffraction peaks are observed for (010), (11-1), (111), (020), (200), (20-1), and (220) planes, with diffraction angles ( $2\theta$ ) being 16.10, 27.90, 30.30, 32.53, 33.70, 36.15, and 47.49°, respectively. Compared to the phase of GTO, Yb,Ho:GYTO crystal is found to show coincident diffraction peaks as GTO, which means that they belong to the same monoclinic space group of  $I_{2/a}$  (No.15).

The concentrations of doping elements Yb, Ho, and Y in the as-grown crystal are shown in Table 1. The  $k_{eff}$  of elements Yb, Ho, and Y are calculated according to the equation  $k_{eff} = C_s/C_0$ , where  $C_s$  and  $C_0$  are the ion concentrations in the crystal and melt, respectively.<sup>18</sup> The effective segregation has close relationship with the ionic radius of doping and host ions. Closer the ionic radius of doping and host ions, easier the host ions can be substituted.<sup>19,20</sup> The ionic radius of doping ions Yb<sup>3+</sup>, Ho<sup>3+</sup>, and Y<sup>3+</sup> is 0.86, 0.89, and 0.94 Å, respectively, which are close to the radius of Gd<sup>3+</sup> 0.89 Å. The  $k_{eff}$  of Yb, Ho, and Y in Yb,Ho:GYTO crystal is 1.08, 0.96, and 0.9, respectively, all close to 1. Therefore, the Gd<sup>3+</sup> is easily replaced by doping ions Yb<sup>3+</sup>, Ho<sup>3+</sup>, and Y<sup>3+</sup> and the doping concentration can be high.

**Table 1** Effective segregation coefficients ( $k_{eff}$ ) of Yb, Ho, and Y in Yb,Ho:GYTO crystal.

Element	Starting material (at %)	Crystal (at %)	$k_{eff}(C_s/C_0)$
Yb	0.05	0.054	1.08
Ho	0.01	0.0096	0.96
Y	0.2	0.18	0.9

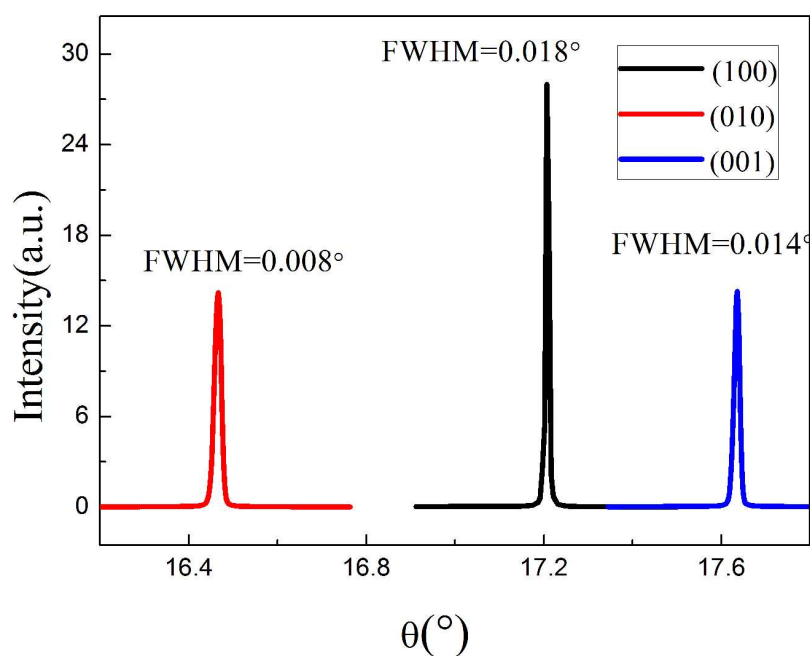


**Fig. 3** X-ray Rocking curves of the (100), (010), and (001) diffraction planes of Yb,Ho:GYTO crystal.

The X-ray rocking curves of the (100), (010), and (001) diffraction planes are shown in Fig. 3. The diffraction peak shows symmetric shape without split and the full width at half maximum (FWHM) is 0.008°, 0.018°, and 0.014°, respectively, which indicates a high crystalline quality for physical property measurements.

### 3.2. Density

The average density of Yb,Ho:GYTO crystal was measured to be  $8.59 \text{ g cm}^{-3}$  by the buoyancy method at room temperature, a little lower than that of GTO ( $8.94 \text{ g cm}^{-3}$ ), mainly resulting from the doping of 20 at%  $\text{Y}^{3+}$  ions. The density values at different temperatures were calculated using the thermal expansion, as presented in Fig. 6. It can be seen that the density of Yb,Ho:GYTO crystal decreases linearly with increasing temperature.

### 3.3 Thermal properties: expansion, specific heat, thermal diffusivity coefficients, and thermal conductivity

The thermal properties are very important parameters for crystal growth and laser performance.<sup>21</sup> For crystals with a monoclinic phase, the thermal expansion coefficient and thermal conductivity are represented by a second-rank symmetric tensor with four independent non-vanishing components.<sup>22,23</sup> However, considering the fact that the samples are limited and in order to make the initial evaluation of the thermal anisotropy, only the thermal expansion coefficients and thermal conductivities along the  $a$ ,  $b$ , and  $c$  axes are measured.

The thermal expansion curves of Yb,Ho:GYTO crystal along three crystalline directions are shown in Fig. 4. The thermal expansions are almost linear in the temperature range of 300-893 K, and the Yb,Ho:GYTO crystal exhibits only positive thermal expansion when heated, which is similar to the GTO crystal. The thermal expansion coefficients along  $a$ ,  $b$ , and  $c$  axes can be calculated according to the formula  $\alpha = \frac{\Delta L}{L_0 \times \Delta T}$ , where  $L_0$  is the sample length at room temperature and  $\Delta L$  is the change of the length in the temperature range  $\Delta T$ .<sup>24</sup> In this case, the average thermal expansion coefficients along  $a$ ,  $b$ , and  $c$  axes are  $\alpha_a = 7.21 \times 10^{-6}$ ,  $\alpha_b = 12.41 \times 10^{-6}$ , and  $\alpha_c = 11.50 \times 10^{-6} \text{ k}^{-1}$  from 300 to 873 K, respectively, suggesting the Yb,Ho:GYTO possesses a little small anisotropic thermal expansion ( $\alpha_b/\alpha_a = 1.721$ ) than that of GTO ( $\alpha_c/\alpha_a = 2.17$ ). In addition, the thermal expansion coefficient along  $a$  axis is smaller than those along the other directions. Thus, it suggests that the Yb,Ho:GYTO crystal grown along  $a$ -axis could effectively reduce the internal stress and the cracking because of the smaller isotropic contraction when cooled, which has been proven by the previous crystal growth part.

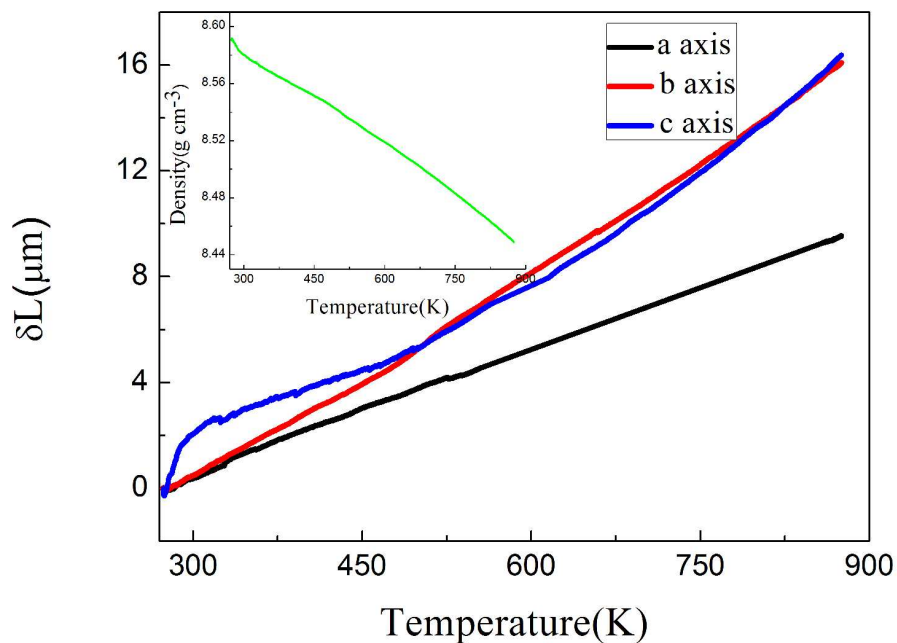


**Fig. 4** Temperature dependent thermal expansion curves of Yb,Ho:GYTO crystal along different directions. Inset: Density versus temperature curve

The specific heat has a significant influence on optical damage threshold of a material in a pulsed laser system. Fig. 5 shows the specific heat as a function of temperature. The specific heat increases with increasing temperature, indicating more tolerance of thermal energy at higher temperature. The values of specific heat is  $0.32 \text{ J (g K)}^{-1}$  at 300 K, which is larger than that of pure GTO ( $0.27 \text{ J (g K)}^{-1}$ ).<sup>13</sup>

The thermal diffusivity of the as-grown crystals are shown and plotted against temperature in Fig. 6. The thermal diffusivity along the *a* and *c* axes are greatly close to each other and greater than those along the *b* axis. The thermal diffusivity decreases with increasing temperature. From Fig. 6, the thermal diffusivity values along the *a*, *b*, and *c* axes are  $2.019$ ,  $1.611$ , and  $2.084 \text{ mm}^2 \text{ s}^{-1}$  at 300 K, respectively.

The thermal conductivity  $k$  can be obtained by measuring the specific heat  $C_p$ , and thermal diffusivity  $\lambda$ , according to the equation  $k = \lambda\rho C_p$ . The variation of thermal conductivity is shown in Fig. 7. The variation of thermal conductivity with increasing temperature is similar to the thermal diffusivity, and the thermal conductivity along the *b* axis is smaller than those along *a* and *c* axes. From Fig. 7, the thermal conductivity values along the *a*, *b*, and *c* axes are  $5.550$ ,  $4.428$ , and  $5.728 \text{ W (m K)}^{-1}$  at 300 K, respectively, a little smaller than that of GTO crystal, which should be ascribed to the more doping ions in the Yb,Ho:GYTO lead to the decreasing crystal order degree and increasing lattice malformation.<sup>25</sup>

It is well known that the phonon density increases with increasing temperature, due to the increased lattice thermal vibrations. The phonon mean free path decreases, which manifests itself as a decrease in the thermal diffusivity and thermal

conductivity.<sup>23,26</sup> Moreover, the thermal diffusivity along the  $c$  axis is larger than those of the other two directions at the same temperature, which indicates that the Yb,Ho:GYTO crystal should be pumped along  $c$ -axis more favorable to reduce the thermal lensing effect.

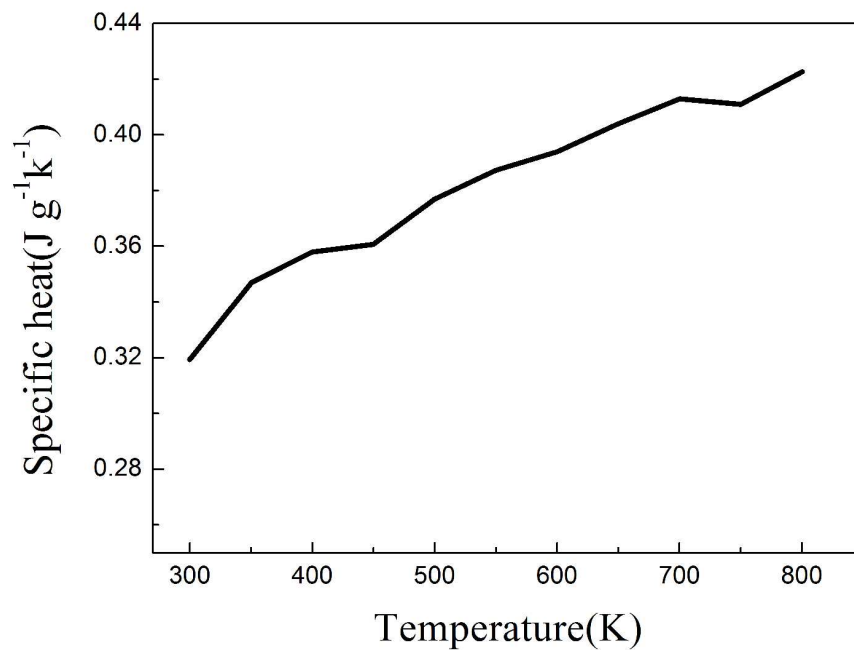


**Fig. 5** The specific heat versus temperature of Yb,Ho:GYTO crystal

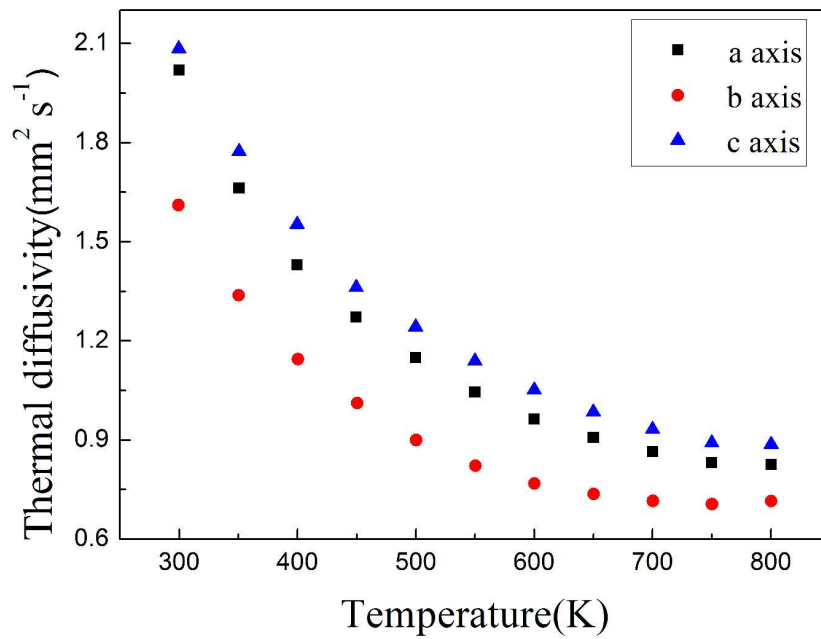


**Fig. 6** Thermal diffusivity coefficients along different detections of the Yb,Ho:GYTO crystal versus temperature.

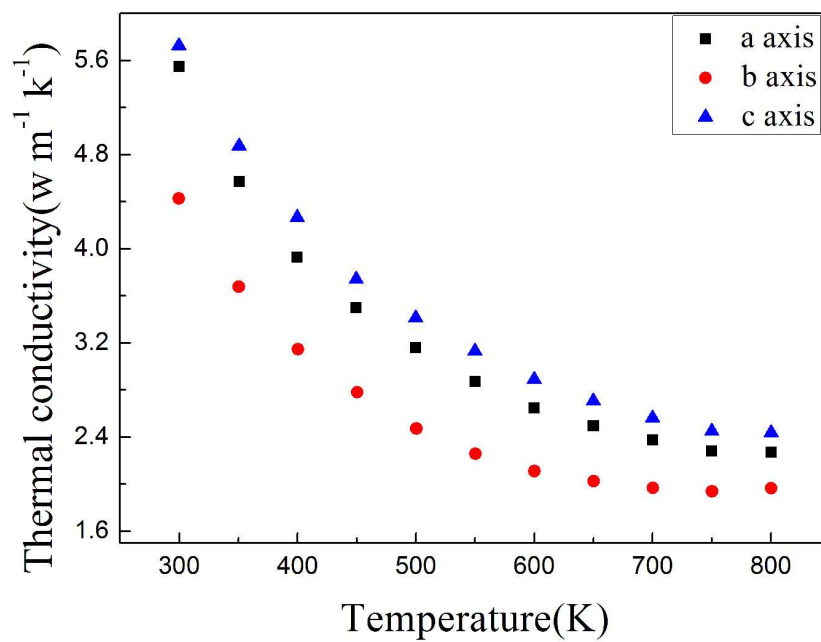


**Fig. 7** Calculated thermal conductivities along different directions of the Yb,Ho:GYTO crystal versus temperature.

### 3.4 Absorption spectra

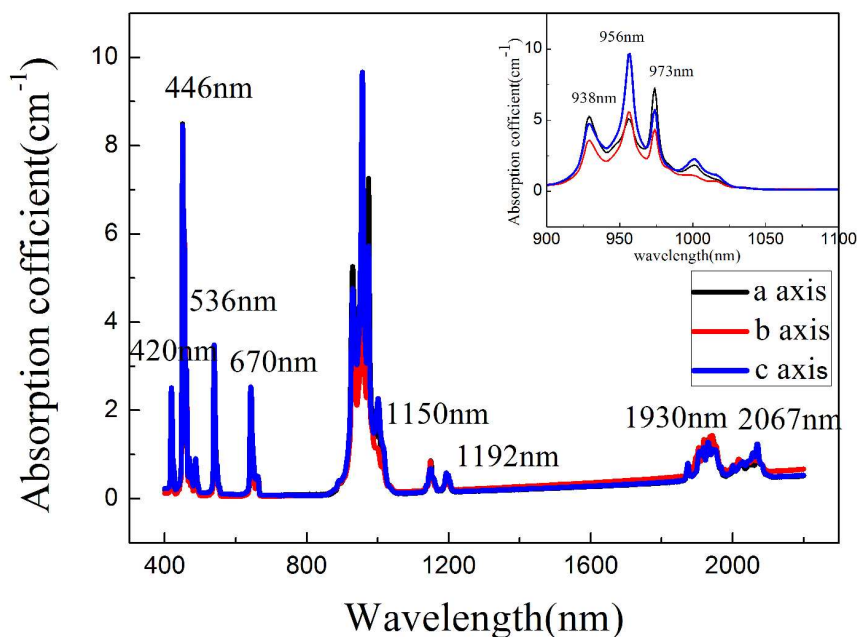


**Fig. 8** Absorption spectra of the Yb,Ho:GYTO crystal along different directions. Inset: Enlarged curve in the range of 900-1100 nm.

Fig. 8 shows the absorption spectra of Yb,Ho:GYTO crystal along *a*, *b*, and *c* axes in the wavelength range of 400-2000 nm. The main absorption bands centered at 420, 446, 536, 670, 1150, 1192, 1930, and 2067 nm are typical absorption transitions of Ho<sup>3+</sup> ions. We are interested in the bands from 900 to 1000 nm, as shown in the insert of Fig. 8, which is the typical absorption of Yb<sup>3+</sup> ions and well matches with the emission wavelength of commercially available high power InGaAs laser diodes (LD). Moreover, as shown in Fig. 8, the absorption coefficient along *c* axis is larger than those along the other directions. It indicates that the *c*-axis samples may be more beneficial for the laser performance by improving pumping efficiency.

### 3.5 Luminescence properties

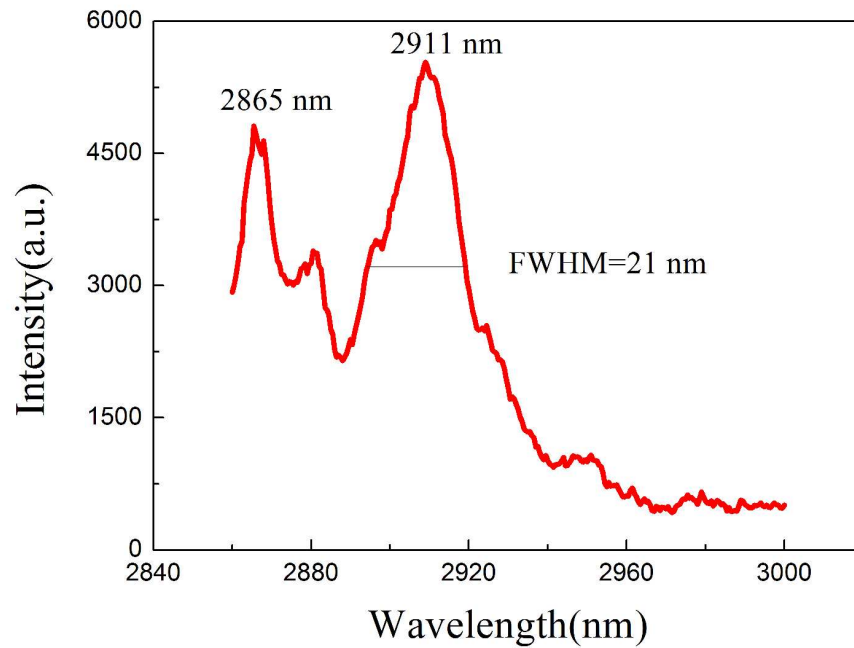
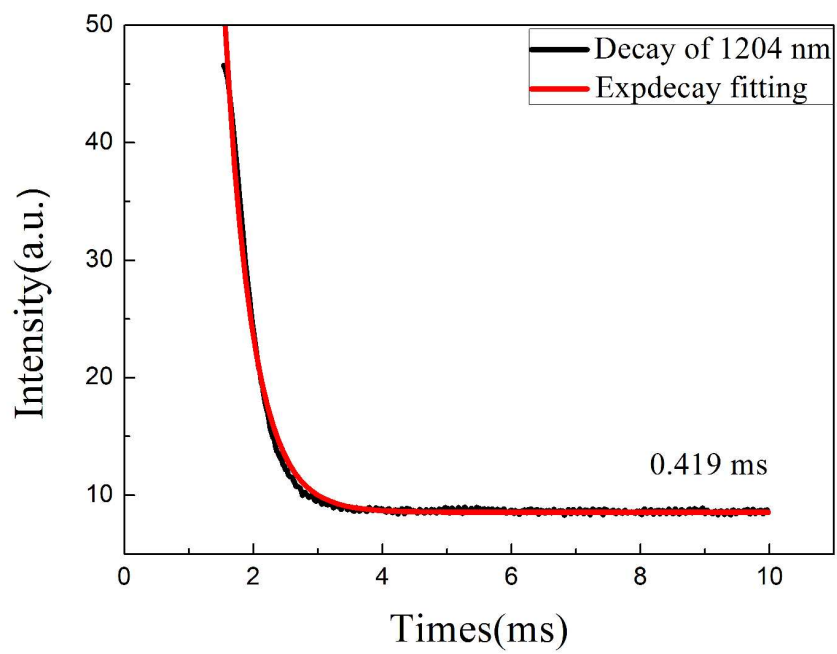
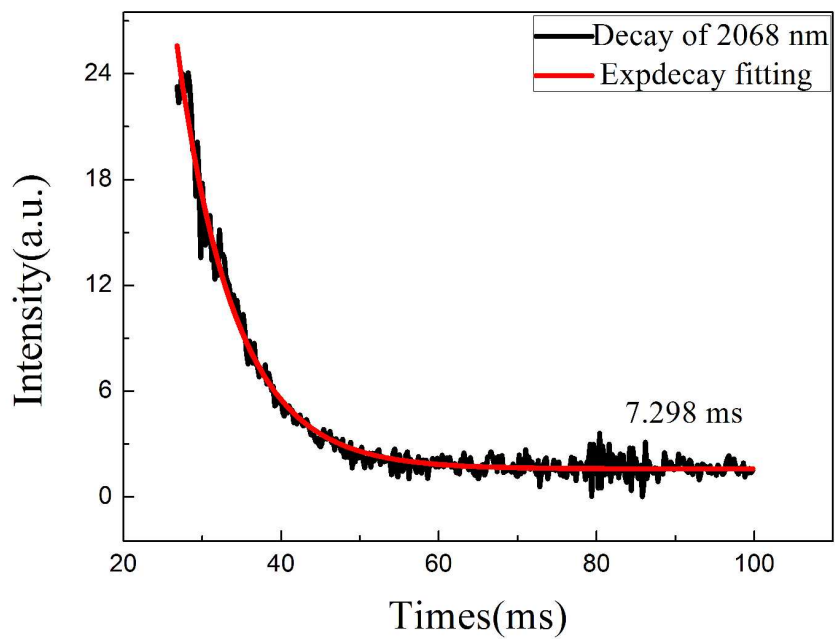


**Fig. 9** Fluorescence spectrum of Yb,Ho:GYTO crystal excited by 940 nm LD.

The fluorescence spectrum of Yb,Ho:GYTO crystal excited by 940 nm LD is shown in Fig. 9. In the range of 2850-3000 nm, two emission bands are observed, centered at 2865 and 2911 nm, which are the typical transitions of stark levels from  $^5I_6$  to  $^5I_7$  of  $\text{Ho}^{3+}$ . The FWHM of the stronger band is 21 nm. This fluorescence spectrum also indicates the energy transfer between  $\text{Yb}^{3+}$  and  $\text{Ho}^{3+}$  ions can be realized successfully.



(a)



(b)

**Fig. 10** Fluorescence decay curves of Yb,Ho:GYTO crystal. (a) 1204 nm decay ( ${}^5I_6 \rightarrow {}^5I_8$ ); (b) 2068 nm decay ( ${}^5I_7 \rightarrow {}^5I_8$ ).

The fluorescence decay curves excited by OPO show single exponential decay behavior, and the lifetimes of upper level and low level are 419  $\mu$ s and 7.298 ms, respectively, as shown in Fig. 7. Compared with the other hosts (shown in Table 2), the Yb,Ho:GYTO exhibits the shorter lifetime of  ${}^5I_7$  and longer lifetime of  ${}^5I_6$ , which are easier to realize population inversion and laser output.

**Table 2** Comparison of the lifetimes of  ${}^5I_7$  and  ${}^5I_6$  in different crystals.

crystal	Ho( ${}^5I_7$ )	Ho( ${}^5I_6$ )
Yb,Ho:YSGG <sup>7</sup>	10.2 ms	585 $\mu$ s
Tm,Ho:LuAG <sup>3</sup>	7.5 ms	250 $\mu$ s
Tm,Ho:YAG <sup>3</sup>	11.4 ms	40 $\mu$ s
Ho:YAG <sup>27</sup>	5.5 $\pm$ 0.5 ms	47 $\pm$ 3 $\mu$ s
Yb,Ho:GYTO (this work)	7.298 ms	419 $\mu$ s

#### 4. Conclusions

A high quality single crystal of Yb,Ho:GYTO with a size of  $\Phi$  23 mm  $\times$  40 mm has been grown by the Cz method successfully. The crystal phase belongs to monoclinic space group of  $I_{2/a}$  (No.15). The  $k_{eff}$  of Yb, Ho, and Y in Yb,Ho:GYTO crystal are 1.08, 0.96, and 0.9, respectively. The thermal expansion coefficients along  $a$ ,  $b$  and  $c$  axes are determined to be  $7.21 \times 10^{-6}$ ,  $12.41 \times 10^{-6}$ , and  $11.50 \times 10^{-6}$   $k^{-1}$ , respectively, which indicates that growth along  $a$ -axis could effectively reduce the internal stress and the crack. The thermal diffusivity values along the  $a$ ,  $b$ , and  $c$  axes are 2.019, 1.611, and 2.084  $mm^2 s^{-1}$  at 300 K, respectively. The thermal diffusivity along the  $c$ -axis is larger than those along the other two directions at the same temperature, which indicates that the Yb,Ho:GYTO crystal should be pumped along  $c$ -axis to reduce the thermal lensing effect. The values of thermal conductivity along the  $a$ ,  $b$ , and  $c$  axes are 5.619, 4.511, and 5.514  $W (m K)^{-1}$  at 300 K. In addition, spectroscopic results show that the 2911 nm emission peak of Ho<sup>3+</sup> can be obtained with Yb<sup>3+</sup> as sensitizer and the FWHM is 21 nm. The absorption coefficient along  $c$ -axis is larger than the other directions also indicates that the  $c$ -axis samples may be more beneficial to the laser performance. Compared with the other hosts, the Yb,Ho:GYTO crystal exhibits a relatively shorter lifetime 7.298 ms for lower laser level  ${}^5I_7$  and longer lifetime 419  $\mu$ s for upper laser level  ${}^5I_6$ , which are very beneficial to realize population inversion and laser output. All the above results indicate that the Yb,Ho:GYTO crystal is a new potential candidate for realizing the 2.911  $\mu$ m laser output pumped by LD.

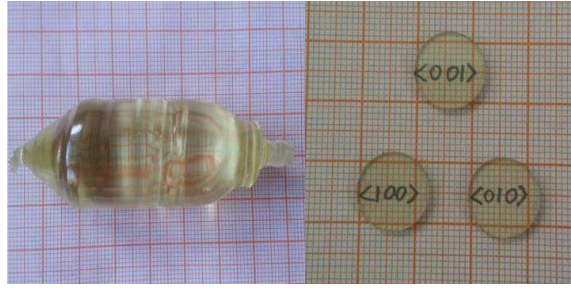
#### Acknowledgments

This work was financially supported by the National Natural Science Foundation of China (Grant Nos. 51172236, 91122021, 51272254, and 61205173).

## References

- 1 M. Tempus, W. Luthy, H. P. Weber, V. G. Ostroumov and I. A. Shcherbakov, *IEEE J. Quantum Elect.* 1994, 30, 2608.
- 2 A. Högele, G. Hörbe, H. Lubatschowski, H. Welling and W. Ertmer, *Opt. Comm.* 1996, 125, 90.
- 3 H. L. Zhang, D. L. Sun, J. Q. Luo, J. K. Chen, S. H. Cao, M. J. Chen, Q. L. Zhang and S. T. Yin, *Acta Optica Sinica*, 2014, 34, 0416006.
- 4 R. C. Stoneman and L. Esterowitz, *Opt. Lett.*, 1992, 17, 816.
- 5 B. J. Dinerman and P.F. Moulton, *Opt. Lett.*, 1994, 19, 1143.
- 6 S. A. Payne, L. K. Smith and W. F. Krupke, *J. Appl. Phys.*, 1995, 77, 4274.
- 7 D. W. Chen, C. L. Fincher, T. S. Rose, F. L. Vernon and R. A. Fields, *Optics Letters*, 1999, 24, 385.
- 8 J. S. Liu, J. J. Liu and Y. Tang, *Laser Phys.*, 2008, 18, 1124.
- 9 Z. J. Zhu, H. Y. Zeng, J. F. Li, Z. Y. You, Y. Wang, Z. X. Huang and C. Y. Tu, *CrystEngComm*. 2012, 14, 7423.
- 10 A. Dening, P. E. A. Moebert, E. Heumann, G. Huber and B. H. T. Chai, *Laser Phys.* 1998, 8, 214.
- 11 A. Dening and S. Kück, *J. Appl. Phys.*, 2000, 87, 4063.
- 12 W. P. Liu, Q. L. Zhang, W. L. Zhou, C. J. Gu and S. T. Yin, *IEEE Trans. Nucl. Sci.*, 2010, 57, 1287.
- 13 H. J. Yang, F. Peng, Q. L. Zhang, C. X. Guo, C. S. Shi, W. P. Liu, G. H. Sun, Y. P. Zhao, D. M. Zhang, D. L. Sun, S. T. Yin, M. Gu and R. H. Mao, *CrystEngComm*. 2014, 16, 2480.
- 14 O. Voloshyna, S. V. Neicheva, N. G. Starzhinskiy, I. M. Zenya, S. S. Gridin, V. N. Baumer, and O. Ts. Sidletskiy, *Materials Science and Engineering B*, 2013, 178, 1491.
- 15 Q. L. Zhang, W. L. Zhou, W. P. Liu, L. H. Ding, J. Q. Luo, S. T. Yin and H. H. Jiang, *Acte Optica Sinica*, 2010, 30, 849.
- 16 H. J. Yang, Q. L. Zhang, P.Y. Zhou, K. J. Ning, J. Y. Gao, Y. He, J. Q. Luo, D. L. Sun and S. T. Yin, *Proc. Of SPIE* , 2011, 8206,1.
- 17 H. J. Yang, Q. L. Zhang, F. Peng, X. F. Wang, J. Y. Gao, J. Q. Luo, D. L. Sun, D. Wang, W. P. Liu and S. T. Yin, *J. Synth. Cryst.*, 2013, 42, 787.

- 18 Z. B. Pan, H. J. Zhang, H. H. Yu, M. Xu, Y. Y. Zhang, S. Q. Sun, J. Y. Wang, Q. Wang, Z. Y. Wei and Z. G. Zhang, *Appl. Phys. B: Lasers Opt.*, 2011, 106, 197.
- 19 Y. Cheng, X. D. Xu, X. B. Yang, Z. Xin, D. H. Cao and J. Xu, *Novel Laser Materials*, 2009, 19, 2133.
- 20 J. D. Fan, H. J. Zhang, J. Y. Wang, Z. C. Ling, H. R. Xia, X. F. Chen, Y. G. Yu, Q. M. Lu and M. H. Jiang, *J. Phys. D: Appl. Phys.* 2006, 39, 1034.
- 21 W. B. Hou, D. Xu, D. R. Yuan, M. G. Liu, N. Zhang, X. T. Tao, S. Y. Sun and M. H. Jiang, *Cryst. Res. Technol.* 1994, 29, 939.
- 22 W. W. Ge, H. J. Zhang, J. Y. Wang, M. H. Jiang, S. Q. Sun, D. G. Ran, H. R. Xia and R. I. Boughton, *J. Appl. Crystallogr.*, 2007, 40, 125.
- 23 X. M. Han, R. Calderon-Villajos, F. Esteban- Betegon, C. Cascales, C. Zaldo, A. Jezowski and P. Stachowiak, *Cryst. Growth Des.*, 2012, 12, 3878.
- 24 Q. Dong, G. J. Zhao, J. Y. Chen, Y. C. Ding and C. C. Zhao, *J. Appl. Phys.* 2010, 108, 023108.
- 25 B. S. Wang, H. H. Jiang, X. D. Jia, Q. L. Zhang, D. L. Sun and S. T. Yin. *Front. Optoelectron. China*, 2008, 1, 138.
- 26 D. H. Sun, Y. H. Leng, Y. H. Sang, X. L. Kang, S. D. Liu, X. Y. Qin, K. Cui, B. K. W. H. Anuar, H. Liu and Y. Bi, *CrystEngComm*. 2013, 15 7468.
- 27 A. C. Larson, R.B.V. Dreele, Los Alamos National Laboratory Report No. LAUR, 2004, 86, 748.



A promising  $2.911 \mu\text{m}$  Yb,Ho:GdYTaO<sub>4</sub> laser crystal has been grown successfully by the Czochralski method for the first time.